FASTEM-4 Validation

Quanhua Liu[1], and others

1. Joint Center for Satellite Data Assimilation, Camp Springs, MD, USA

	FASTEM-4 Validation	Doc ID	: NWPSAF-MO-VS-045
		Version	: 1.0
		Date	: 16 June 2011

This documentation was developed within the context of the EUMETSAT Satellite Application Facility on Numerical Weather Prediction (NWP SAF), under the Cooperation Agreement dated 1 December, 2006, between EUMETSAT and the Met Office, UK. The partners in the NWP SAF are the Met Office, ECMWF, KNMI and Météo France.

Change record			
Version	Date	Author / changed by	Remarks
1.0	16.6.11	Quanhua Liu & others	Version for distribution.

FASTEM-4 VALIDATION

Quanhua Liu, and others

1. Joint Center for Satellite Data Assimilation, Camp Springs, MD
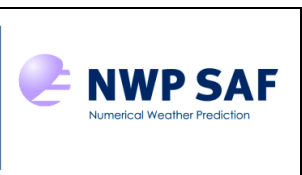
June 16, 2011

[1]Corresponding author address: Dr. Quanhua Liu, Joint Center for Satellite Data Assimilation, Room 703, 5200 Auth Road, Camp Springs, MD 20746, Email: Quanhua.Liu@noaa.gov

1.1.1.1 Abstract

A fast microwave emissivity model (FASTEM), which was developed by the Met office (United Kingdom) has been extended as FASTEM-4 within the collaboration between the Met Office at the United Kingdom and the Joint Center for Satellite Data Assimilation (JCSDA) at the United State. In the FASTEM-4, a new permittivity model is generated by using the measurements for fresh and salt water at frequencies between 1.4 GHz and 410 GHz. A modified sea surface roughness model from Durden and Vesecky is applied to the detailed two-scale surface emissivity calculations. The two-scale model simulates azimuthal variation of the sea surface emissivity, therefore the model is applicable in determining wind direction. This report documents the change of the FASTEM-4. The amplitude parameter for small-scale reflection in two-scale model is tuned. The foam coverage is changed back to use Monahan et al.(1986), as used in FASTEM-1, 2,and 3. A look-up table is used to replace the regression equation for large-scale part. The revised FASTEM-4 is validated using the match-up data set for Aqua AMSR-E and MHS from Ralf Bennartz at the University of Wisconsin, collocated satellite data and ECMWF model data from the NOAA Microwave Integrated Retrieval System (MiRS, Sid Boukabara), and the NOAA NCEP GSI system. The results show that FASTEM-4 has much better performance in comparison to previous FASTEM versions.

1.   **Introduction**

Ocean emissivity at a given frequency is affected by surface wind speed, wind direction, water salinity, temperature, and viewing angles. In addition, wind stage, whether in developing or developed, and surface stability can also effect surface emissivity calculations. For a flat water surface, the reflectance can be accurately calculated from Fresnel formula for a given water permitivity and a local incident angle. When the ocean surface becomes rough, surface reflection of radiation will be contributed by various scales of ocean waves such as gravity and capillary waves. For a wind speed larger than 7 ms^{-1} whitecap occurs leading to surface foam and this modifies the surface reflection. For fast computations of ocean reflectivity or emissivity, a model called FASTEM (FAST microwave Emissivity Model) was developed and is used in remote sensing and data assimilation communities [1]. FASTEM uses small-scale correction factor to modify Fresnel reflection coefficients. In FASTEM-1, the fitting coefficients for large-scale part were based on geometric optics (GO) theory [2]. In the GO model, surfaces modulated by a large scale wave are treated as an ensemble of facets, for which the Fresnel formula can be applied individually. The total reflectivity is then obtained by averaging the Fresnel reflection coefficients of the individual facets weighted with the slope probability density distribution [3]. The GO model is a first order approximation and the accuracy of derived emissivity is not adequate for some microwave remote sensing applications. The GO model also lacks of coherent and incoherent interactions in the bistatic scattering coefficients, which do not produce the fourth Stokes component.

FASTEM-2 is the same as FASTEM-1, except for that atmospheric transmittance may be used to adjust surface reflectance for from surface reflected downward flux. It was found that such adjustment may be necessary if downward radiation is significant and strongly depends on zenith angle. The adjustment has to be switched off when multiple directional radiation streams are used.

The FASTEM 3 updated fitting coefficients and included azimuthal components for specific sensor, WindSat. FASTEM 1, 2, and 3 don't include salinity, therefore users need aware of the application at low frequencies.

FASTEM-4 is generic, applicable for all passive microwave instruments. A rigorous two-scale surface emissivity model has been developed to include the small-scale wave and the interactions [5][6]. The two-scale model takes the same facet treatment as the GO model for the large-scale wave, but uses the bistatic scattering coefficients instead of the modified Fresnel reflection coefficients. The coherent part of the bistatic scattering coefficients is a sum of the Fresnel reflection coefficients and the correction of the specular reflection coefficients caused by the small surface perturbation that depend on the shortwave part of the surface roughness spectrum [4]. The incoherent scattering coefficients are proportional to the shortwave part of the surface roughness spectrum. This study incorporate into FASTEM the full accuracy obtained by the two-scale model along with the full surface roughness spectrum model [7], an accurate permittivity model (see Figure 1 and Table 1) and a foam model [8].
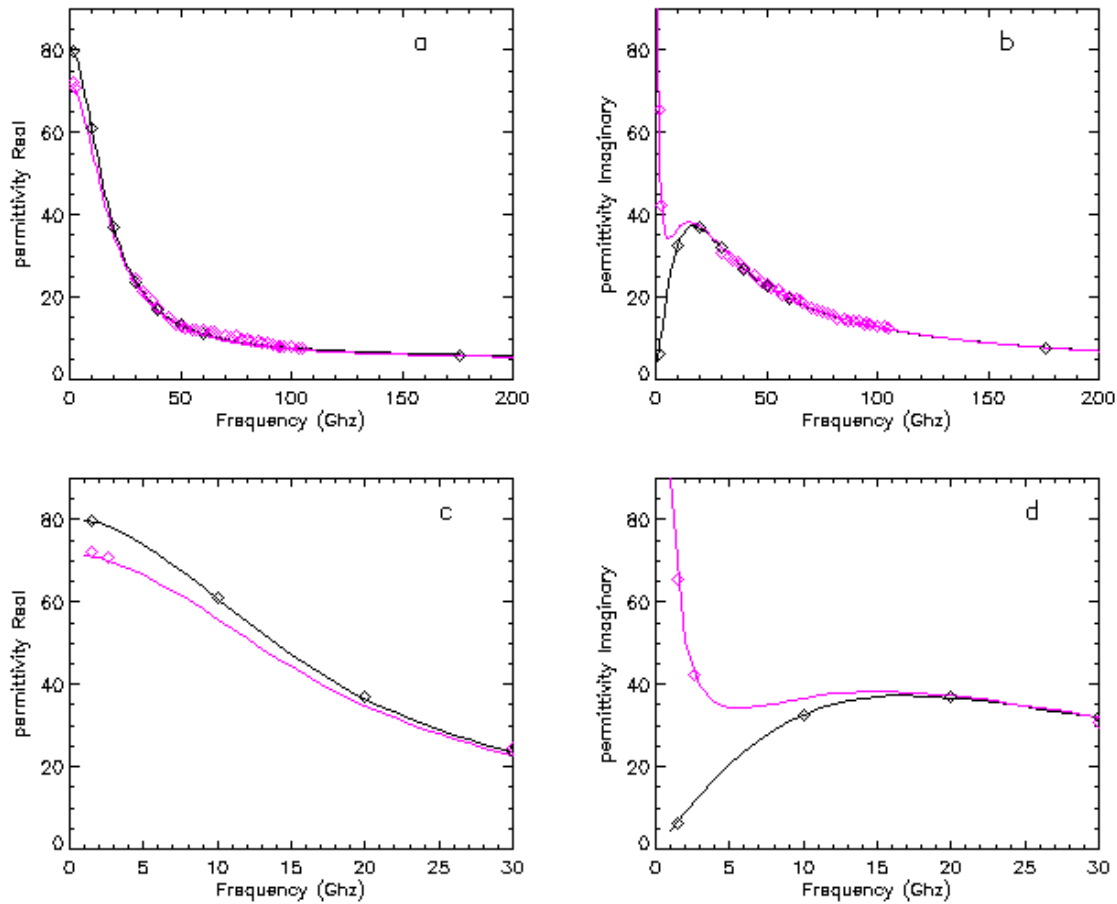
Figure 1. Panels (a) and (b) represent the real and imaginary parts of the permittivity. Panels (c) and (d) are a zoom-in part for low frequencies. The back line is for fresh water and the red line is for salted water. The water temperature is 25˚C. The salinity of sea water is 35‰. The solid lines represent model results. The diamond symbols are for measurements.

Table 1. Comparisons of water permittivity between measurements and calculations using the permittivity model of the OEMM/FASTEM-4, Klein and Swift (1977), Guillou et al. (1998), Meissner and Wentz (2004), and Ellison et al. (2003).

	Salted and fresh water				fresh water			
	real		imaginary		real		imaginary	
	bias	rms	bias	rms	bias	Rms	bias	rms
FASTEM4 model	0.62	0.91	-0.04	0.50	-0.04	0.35	0.00	0.35
Klein and Swift, 1977	1.01	1.39	-0.34	0.86	0.02	0.44	-0.09	0.58
Guillou et al., 1998	0.15	1.43	-1.06	1.78	-0.23	2.05	-0.40	2.30

Meissner and Wentz, 2004	0.81	1.44	0.10	0.52	-0.02	0.34	0.00	0.35
Ellison et al. (2003), S=35‰ f > 20 GHz	1.24	1.52	-0.41	0.91	0.09	0.41	-0.12	0.64

2.   Foam Effects

For a wind speed larger than several meters per second, foam starts to affect the surface emissivity. Foam is often a mixture of air and water. The air volume fraction in the foam can be very high, greater than 0.95. The foam coverage may be expressed by [36]:

$$f_c = a\left(\frac{V}{V_0}\right)^b,$$ (1)

where V is the wind speed in $m\,s^{-1}$ at 10 meter above sea surface and V_0 is a constant of 1 $m\,s^{-1}$. The total reflectivity is calculated from the sum of the foam reflectivity weighted with the foam coverage (f_c) and the reflectivity of water weighted with the water coverage ($1 - f_c$).

Both foam emissivity and coverage affect the surface emissivity and the two parameters may also depend on the stability in a lower boundary layer. Schrader [37] explicitly treat sea foam as the third scale in his microwave ocean emissivity model and investigated 9 foam coverage models. In FASTEM 1, 2, and 3, Monahan et al. (1986) foam coverage model is applied without surface stability term. The foam coverage was for wind speeds between 1 and 15 m/s. The foam coverage formula from Tang [1974] was stated applicable for wind speeds below 35 m/s. Figure 2 shows the foam coverage from Tang [1974] and Monahan et al. (1986). The foam coverage from Tang [1974] for large wind speed is too large. In the revised FASTEM-4, we will use the foam coverage from Monahan et al. (1986).
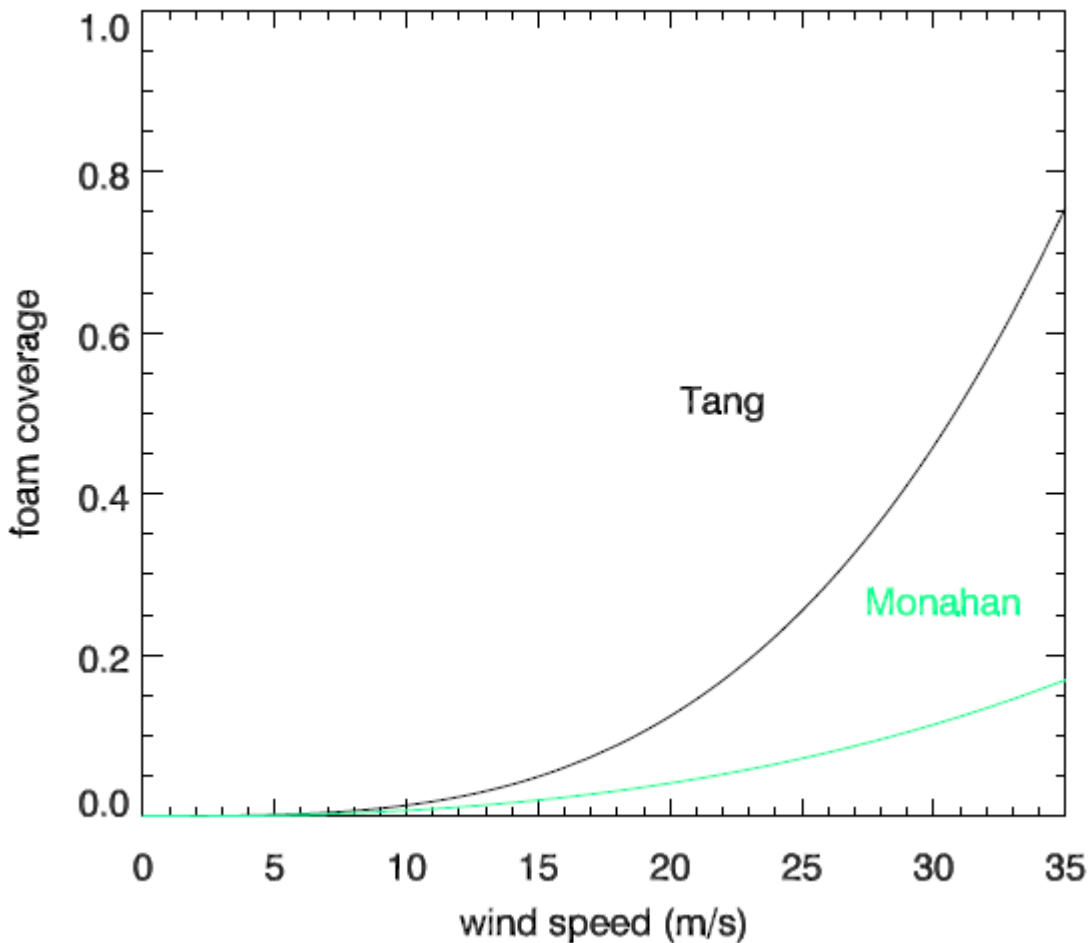
Figure 2. Foam coverage as a function of wind speeds.

3. **Reflectance Coefficients**

The detailed two-scale modeling of the ocean surface emissivity [5][6][33] require integrations over the ocean wave spectrum and over all facet directions, which demand large computational resources. The detailed two-scale model usually serves as an accurate model to derive an approximate and fast emissivity model, such as FASTEM. In the FASTEM-4, the emissivity for a zenith angle θ and a relative azimuth angle ϕ_R at the surface thus can be summarized as follows:

$$E_v = (1 - f_c)[1 - F_v \exp[-y \cos^2 \theta)] + L \arg e\_cor_v] + f_c \times E_{foam\_v} + \sum_{m=1}^{3} c_m \cos(m\phi_R) , \qquad (2a)$$

	FASTEM-4 Validation	Doc ID : NWPSAF-MO-VS-045
NWP SAF Numerical Weather Prediction		Version : 1.0
		Date : 16 June 2011

The EUMETSAT Network of Satellite Application Facilities

$$E_h = (1 - f_c)[1 - F_h \exp[-y\cos^2\theta)] + L\arg e\_cor_h] + f_c \times E_{foam\_h} + \sum_{m=1}^{3} d_m \cos(m\phi_R), \qquad (2b)$$

$$E_3 = \sum_{m=1}^{3} e_m \sin(m\phi_R), \qquad (2c)$$

$$E_4 = \sum_{m=1}^{3} g_m \sin(m\phi_R). \qquad (2d)$$

where the small-scale correction parameter $y = h(k\xi_c)^2$ [31], large-scale correction terms $L\arg e\_cor_v$ and $L\arg e\_cor_h$, are determined by fitting the rigorous two-scale model calculations. The coefficients c_m, d_m, e_m, g_m are obtained by fitting both surface measurement data and the rigorous two-scale model calculations, which enables us to apply the azimuthal part to various zenith angles and frequencies. The effects of sea foam on the emissivity for the third (E_3) and the fourth (E_4) Stokes components are not explicit and may be partially included by fitting the measurement data.

In the FASTEM-4 model, the small-scale correction parameter y was set to the surface wind speed. In this study, we use the following regression equation for the small-scale correction parameter:

$$y = h_1 \times W \times f + h_2 \times W \times f^2 + h_3 \times W^2 \times f + h_4 \times W^2 \times f^2 + h_5 \times W^2 / f + h_6 \times W^2 / f^2 + h_7 \times W + h_8 \times W^2 . (3)$$

where wind speed W is given in meter per second and frequency is given in GHz. The coefficients h_i are obtained by fitting the surface height variance that can be computed from the surface roughness. Figure 6 shows the comparison of y between the detailed surface roughness calculation and the calculation using the regression equation (14). The two results agree very well.
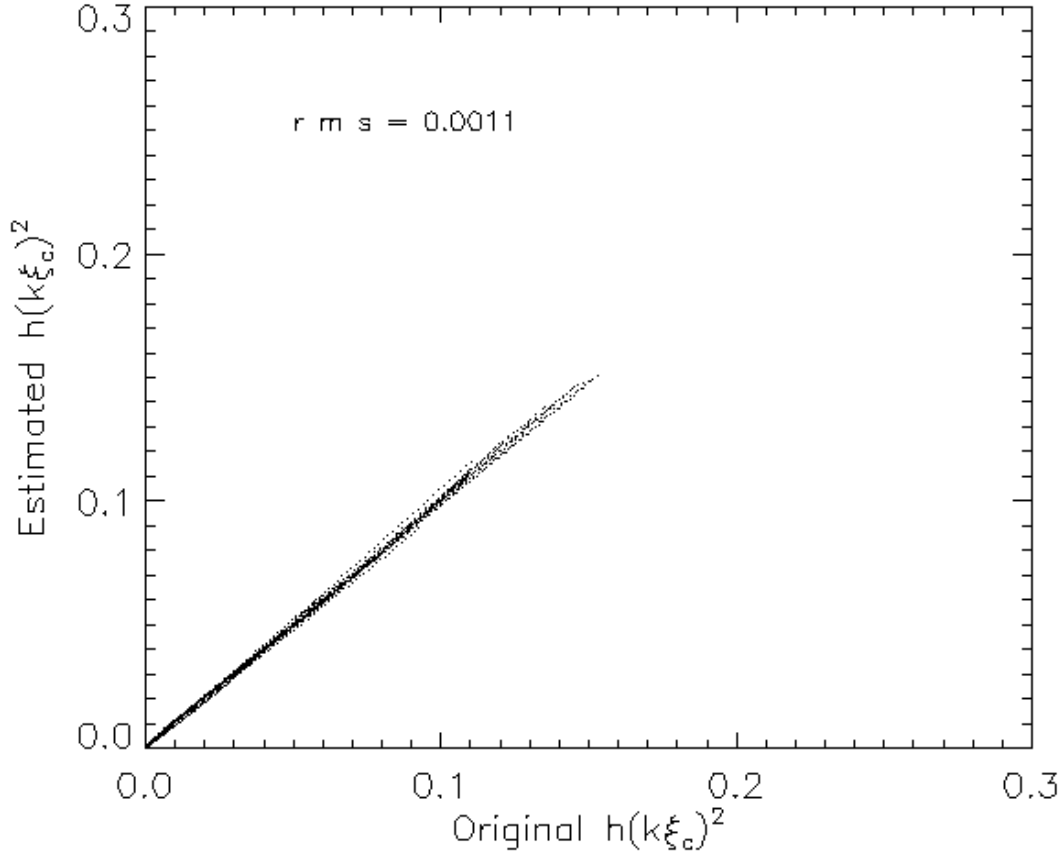
Figure 3. Comparison of the small-scale correction parameter (see Eq.(2a-b)) between detailed surface roughness spectrum calculation and the regression calculation in Eq.(3).

The large-scale correction parts are written in the following regression equations:

$$
\begin{aligned}
L \arg e\_cor_v = z_1 + z_2 f + z_3 f^2 + (z_4 + z_5 f + z_6 f^2)/\cos\theta + (z_7 + z_8 f + z_9 f^2)/\cos^2\theta \\
+ (z_{10} + z_{11}f + z_{12}f^2)\times W + (z_{13} + z_{14}f + z_{15}f^2)\times W^2 + (z_{16} + z_{17}f + z_{18}f^2)\times W/\cos\theta
\end{aligned}
,(4a)
$$

$$
\begin{aligned}
L \arg e\_cor_h = z_{19} + z_{20}f + z_{21}f^2 + (z_{22} + z_{23}f + z_{24}f^2)/\cos\theta + (z_{25} + z_{26}f + z_{27}f^2)/\cos^2\theta \\
+ (z_{28} + z_{29}f + z_{30}f^2)\times W + (z_{31} + z_{32}f + z_{33}f^2)\times W^2 + (z_{34} + z_{35}f + z_{36}f^2)\times W/\cos\theta
\end{aligned}
.(4b)
$$

The regression coefficients z_i are evaluated using the large-scale contribution extracted from the rigorous two-scale model calculations with a constraint to ensure the same emissivity value for both vertical and horizontal polarization at nadir.

4. **Fitting Coefficients**

We keep the azimuthal emissivity part and small-scale correction unchanged. Thus, by subtracting above parts from total emissivity in Eqs.(2a-b), we get the large-scale part. Using regression Eq.(4a-b), we can derive the fitting coefficient z_i. As shown in Table 2, bias for vertically polarized emissivity is relatively small, except at 10 and 50 GHz. The bias for horizontally polarized emissivity is significant, for example 0.02 bias can lead a systematic error of 5 K at the top of the atmosphere. We haven't found better fitting method yet. This update will use a look-up table technique for the large-scale part.

Table 2. Regression accuracy for large-scale part fitting.

Frequency	vertical-polarized		horizontal-polarized	
	Bias	rms	bias	rms
1.40	0.00026	0.00869	0.00205	0.00425
6.60	−0.00594	0.01514	−0.01079	0.01366
10.70	−0.01225	0.02510	−0.02341	0.02937
18.70	−0.00062	0.00696	−0.00209	0.00613
19.35	0.00037	0.00694	−0.00088	0.00525
22.23	0.00448	0.01040	0.00449	0.00714
23.80	0.00640	0.01316	0.00736	0.01038
31.40	0.00028	0.00993	−0.00053	0.00683
37.00	−0.00267	0.01059	−0.00427	0.00901
50.00	0.01216	0.03271	0.02770	0.03908
53.00	0.00778	0.02737	0.02111	0.03181
55.00	0.00528	0.02432	0.01717	0.02718
85.00	−0.00457	0.02168	−0.01204	0.02043
89.00	−0.00652	0.02396	−0.01589	0.02422
150.00	−0.00784	0.02107	−0.01744	0.02409
157.00	−0.00670	0.01800	−0.01526	0.02074
183.31	0.00309	0.01137	0.00675	0.01055
190.31	0.00700	0.01848	0.01597	0.02109

5. **Comparison Result**

This comparison has been carried out for the Aqua AMSR-E and MHS match-up data, provided by Ralf Bennartz at the University of Wisconsin. It is for 2006-2007 period and all data used here are over oceans and most-likely clear sky. The clear-sky cases are determined by CloudSat

measurements. The Aqua AMSR-E has 12 channels between 6.9 and 89 GHz. The zenith angle is 55º for this conical scan instrument. Atmospheric temperature and water vapor profiles as well as sea surface temperature are taken from the ECMWF model outputs. The Community Radiative Transfer Model is applied here. The result should be very close to that using RTTOV because the transmittance difference from the two models is negligible in the microwave region. Table 3 summarizes the comparison result for using FASTEM-1, 3, and 4, respectively. For conical instrument, the error using the FASTEM-1 is very large, in particular at low frequencies. The performance using the FASTEM-3 at low frequencies is good, but dramatically degraded as the frequency increases. The FASTEM-4 has the best performance here.

Table 3. Comparison between satellite observed and using various emissivity models simulated Aqua AMSR-E brightness temperatures. The transmittance and relative azimuth angle options are switched off, therefore the FASTEM-1 and 2 are the same. The bias is defined as observation minus simulation.

Frequency	N	FASTEM-1 (K) bias	rms	std	FASTEM-3 bias	rms	std	FASTEM-4 bias	rms	std
6.92	93587	−11.95	12.11	1.93	0.29	0.95	0.91	−0.38	0.95	0.87
6.92	93587	−20.14	20.84	5.33	−0.54	0.93	0.76	0.10	1.08	1.07
10.65	111341	−8.04	8.09	0.91	0.31	1.00	0.95	−0.30	0.97	0.92
10.65	111341	−14.03	14.36	3.06	−0.09	1.10	1.10	0.56	1.56	1.45
18.70	122224	−4.45	4.57	1.01	0.30	1.11	1.07	0.37	1.33	1.27
18.70	122224	−6.66	6.82	1.46	1.94	2.51	1.58	−0.16	1.14	1.12
23.80	122224	−2.97	3.22	1.23	0.32	1.25	1.21	0.22	1.36	1.35
23.80	122224	−2.71	3.19	1.67	3.59	4.16	2.10	0.78	1.56	1.34
36.50	122224	−3.53	3.74	1.23	0.24	1.30	1.28	0.77	1.81	1.64
36.50	122224	−3.31	3.90	2.06	4.72	5.54	2.89	−0.05	2.12	2.12
89.00	122224	0.10	2.08	2.08	1.52	2.67	2.19	1.04	2.53	2.31
89.00	122224	2.20	4.58	4.01	6.73	8.48	5.16	0.65	3.84	3.79

For the NOAA-18 MHS observations at nadir, both FASTEM-1 and FASTEM-4 obtained good results (see Table 4). The error using FASTEM-3 is large.

Table 4. Comparison between satellite observed and using various emissivity models simulated NOAA-18 MHS brightness temperatures. The transmittance and relative azimuth angle options are switched off, therefore the FASTEM-1 and 2 are the same. The bias is defined as observation minus simulation.

Frequency		FASTEM-1 (K)			FASTEM-3			FASTEM-4		
	N	bias	rms	std	bias	rms	std	bias	rms	std
89.0	8003	1.40	3.29	2.97	4.48	5.59	3.34	0.62	2.96	2.89
157.0	8003	1.16	2.34	2.03	2.03	3.15	2.41	0.90	2.09	1.89
183.3±1	8003	0.97	2.01	1.75	0.97	2.01	1.75	0.97	2.01	1.75
183.3±3	8003	0.51	1.38	1.28	0.51	1.38	1.28	0.51	1.38	1.28
190.3	8003	−0.23	1.00	0.97	−0.20	1.02	1.00	−0.24	0.99	0.96

The NOAA Microwave Integrated Retrieval System (MiRS, Sid Boukabara et al. 2007) provides routinely retrieval products and satellite observations and ECMWF (also NCEP GDAS) collocated data sets. The MiRS system treats surface emissivity as retrieval variables. It does not apply any surface emissivity model. In this study, we use the retrieved cloud water content to determine clear-sky cases. Table 5 lists the bias, rms error and standard deviation for May 04, 2011. The result is similar for May 07, 2011. The error using FASTEM-3 is large. The FASTEM-1 for the AMSU has good performance. The FASTEM-4 has better performance, in general.

Table 5. Comparison between satellite observed and using various emissivity models simulated NOAA-18 AMSU-A + MHS brightness temperatures. The transmittance and relative azimuth angle options are switched off, therefore the FASTEM-1 and 2 are the same. The bias is defined as observation minus simulation.

AMSU-A	FASTEM-1 (K)			FASTEM-3			FASTEM-4		
F	bias	rms	std	bias	rms	std	bias	rms	std
23.8	−1.23	2.71	2.42	2.39	3.47	2.51	0.75	2.67	2.57
31.4	−2.46	2.86	1.46	2.14	2.67	1.59	−0.25	1.84	1.83
50.3	0.11	1.50	1.50	2.28	2.82	1.66	0.58	1.80	1.71
52.8	−0.77	1.11	0.81	−0.34	0.98	0.91	−0.65	1.07	0.84
53.6	−0.77	0.94	0.53	−0.70	0.90	0.56	−0.74	0.92	0.54
89.0	0.35	2.46	2.44	2.75	3.87	2.72	0.27	2.54	2.52
	MHS								
89.0	0.12	2.58	2.58	2.51	3.81	2.86	0.04	2.68	2.68
157.0	0.06	1.52	1.52	0.48	1.81	1.75	0.04	1.53	1.53
183.3	−0.31	1.67	1.64	−0.31	1.67	1.64	−0.31	1.67	1.64
183.3	−0.67	1.47	1.31	−0.67	1.47	1.31	−0.67	1.47	1.31
190.3	−1.02	1.49	1.08	−1.02	1.49	1.08	−1.02	1.49	1.08

The FASTEM models are also tested in the NCEP GSI system for January 15, 2011. We compared the satellite observations and using 6h forecast model data simulated brightness temperatures. The cloud condition is again determined by cloud water content that is estimated using the NOAA-18 AMSU window channels 1 and 2 (Weng and Grody, 1994).
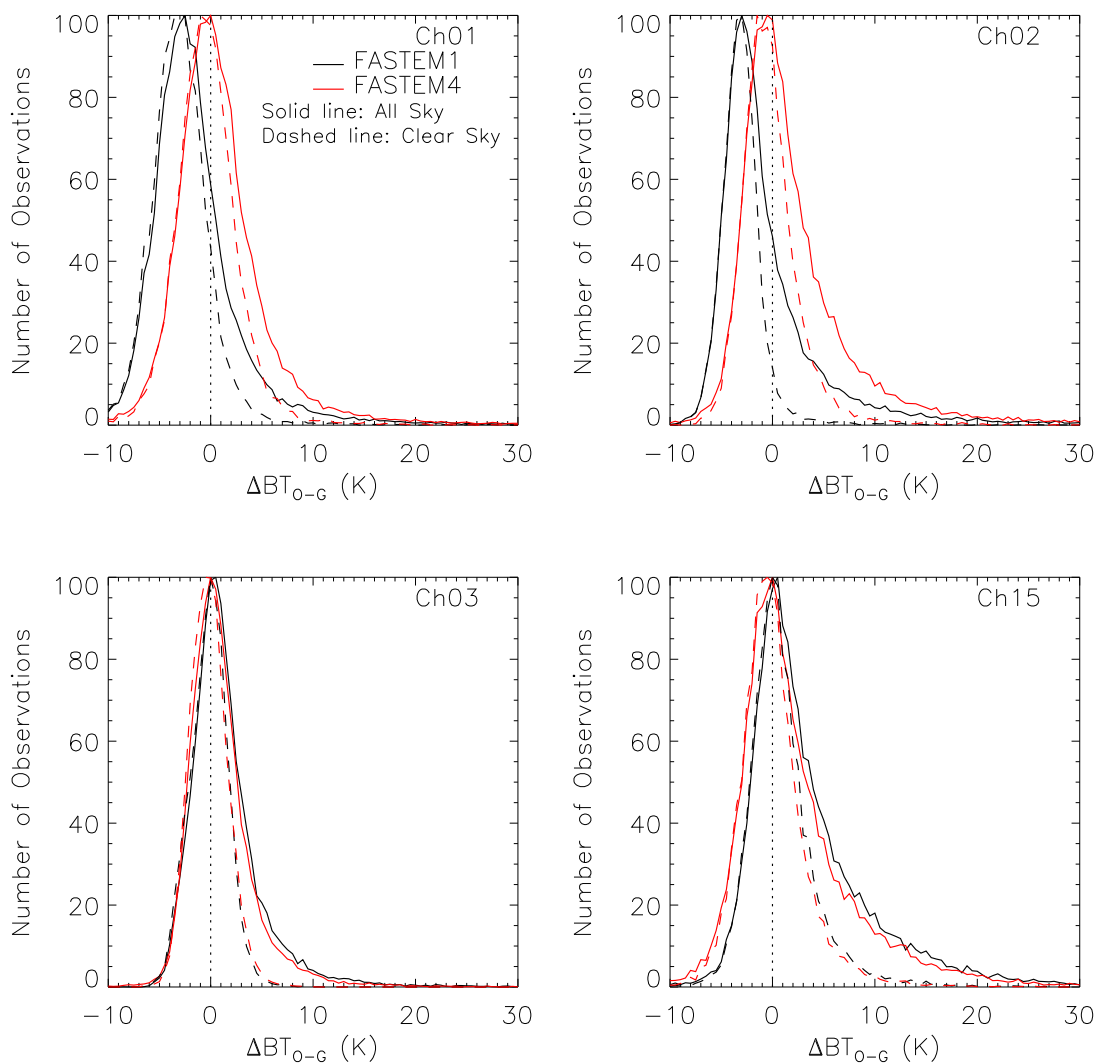

Figure 4. Histogram for the AMSU-A (NOAA-15, 17, 18, 19, Metop-A) brightness temperature difference, observation minus simulations.

6. Discussions

A new permittivity model, a full surface roughness spectrum model, and a rigorous two-scale microwave ocean emissivity model are applied to generate the microwave emissivity over water for various water temperatures, wind speeds, and frequencies. Figure 5 shows the FASTEM-4 can used to study ocean salinity and Figure 6 shows the capability for determining wind direction.
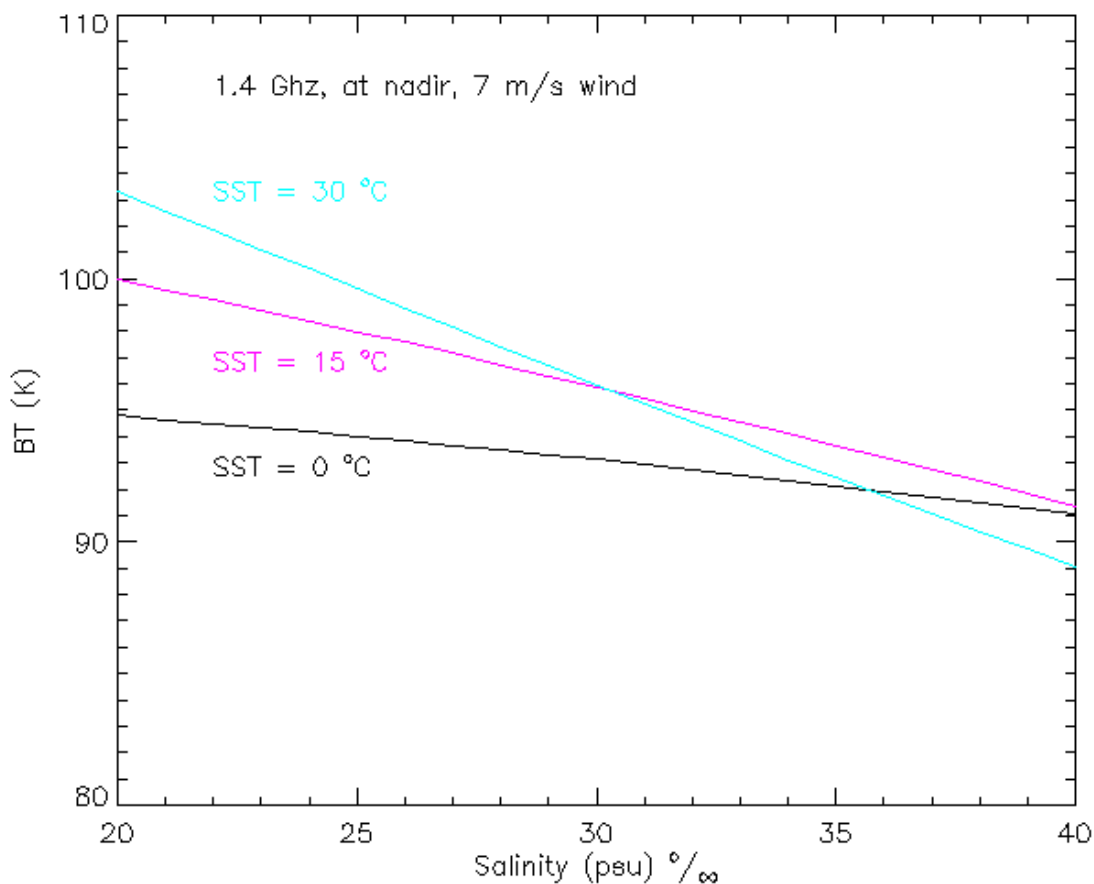

Figure 5. Variation of the surface brightness temperature at 89 GHz and 150 GHz to zenith angles. The sea surface temperature is 12 ˚C and the salinity is 35 ‰. The solid line represents the rigorous two-scale model calculation and the dashed line indicates the OEMM/FASTEM-4 calculation. The green curve is the FASTEM-3 calculation.
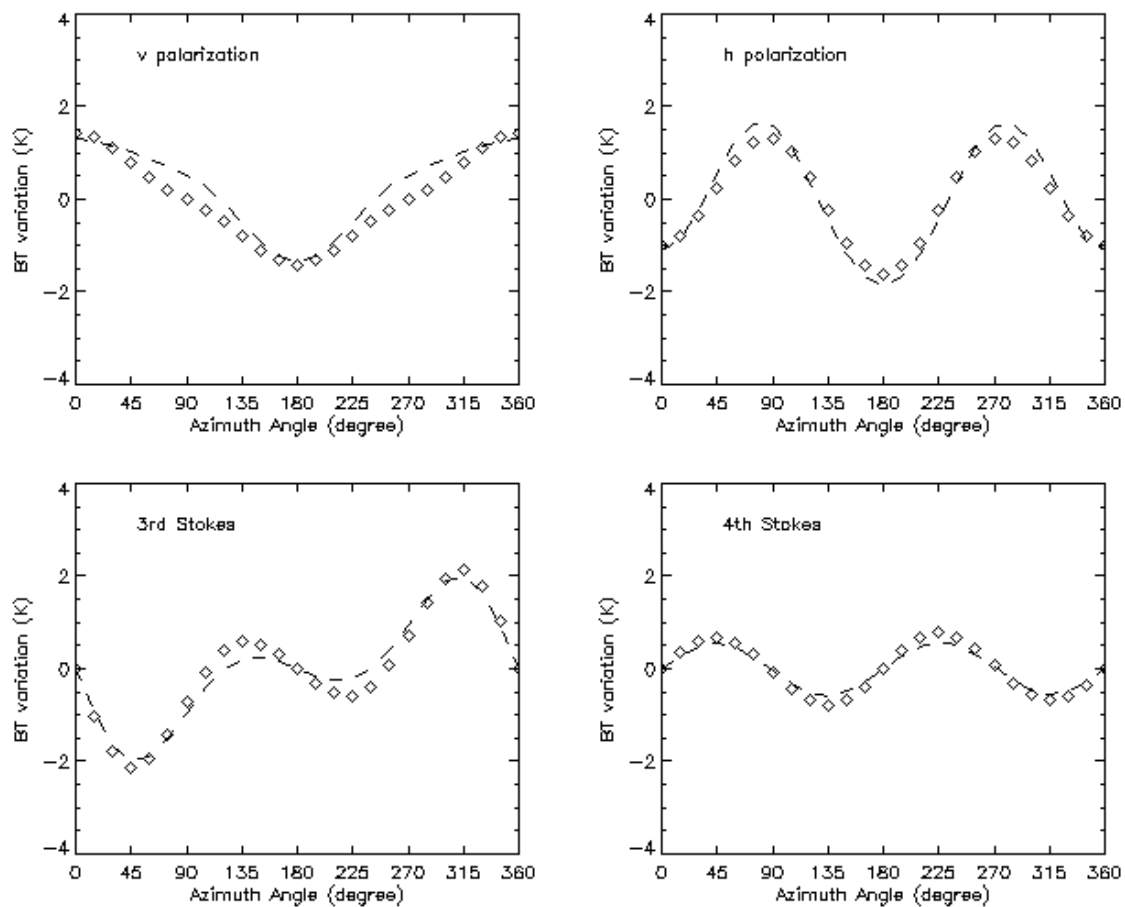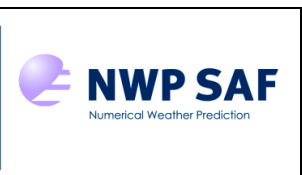
Figure 6. Variation of the surface Stokes vector of the brightness temperature at 19 GHz to azimuth angles (i.e. wind direction for a sensor azimuth angle = 0 degree). The sea surface temperature is 12 ˚C and the salinity is 35 ‰. The surface wind speed at 10 m above the sea surface is 7 ms^{-1}. The dashed line is from the FASTEM-4 calculations and symbol diamond represents two-scale calculations.

FASTEM-1 has good performance for AMSU (mixed polarization), but the error is very large for conical scan sensor (pure polarization). FASTEM-3 obtained good result at low frequency, it dramatically degraded at high frequency. FASTEM-4 has good performance for cross-scan and conical scan sensors at frequency from low to high.

REFERENCE

[1] English, S., and T. Hewison (1998), A fast generic millimeter-wave emissivity model, Proceedings of SPIE, 3503, 288-300.

[2] Stogryn, A. (1967), The Apparent Temperature of the Sea at Microwave Frequencies, *IEEE Trans. Antennas Propagat.*, vol. AP-15, pp. 278–286.

[3] Tsang, L., J. A. Kong, and R. T. Shin, Theory of microwave remote sensing, A Wiley-Interscience Publication, John Wiley & SONS, 613 pp, 1985.

[4] Hollinger, J. P. (1971), Passive microwave measurements of sea surface roughness, *IEEE Trans. Geosci. Electron.*, GE-9, 165–169.

[5] Wu, S. T. and A.K. Fung (1972), A Noncoherent Model for Microwave Emissions and Backscattering from the Sea Surface, *J. Geophys. Res.*, 77, 5971-5929.

[6] Yueh, S. H., S. V. Nghiem, R. Kwok, W. J. Wilson, F. K. Li, J. T. Johnson, and J. A. Kong (1994), Polarimetric thermal emission from periodic water surfaces, *Radio Sci.*, vol. 29,. 87–96, 1994.

[7] Durden, S. P., and J. F. Vesecky (1985), A physical radar cross-section model for a wind-driven sea with swell, *IEEE J. Oceanic Eng.*, OE-10, 445–451.

[8] Kazumori, M., Q. Liu, R. Treadon, and J. C. Derber (2008), Impact study of AMSR-E radiances in the NCEP global data assimilation system, *Mon. Wea. Rev.*, 136, 541-559.

[9] Klein, L. A., and C. T. Swift (1977), An improved model for the dielectric constant of sea water at microwave frequencies, *IEEE Trans. Antennas Propagat.* AP-25, 104–111.

[10] Ellison, W. J., S. J. English, K. Lamkaouchi, A. Balana, E. Obligis, G. Deblonde, T. J. Hewison, P. Bauer, G. Kelly, and L. Eymard (2003), A comparison of ocean emissivity models using the Advanced Microwave Sounding Unit, the Special Sensor Microwave Imager, the TRMM Microwave Imager, and airborne radiometer observations, J. Geophys. Res., 108(D21), 4663, doi:10.1029/2002JD003213

[11] Guillou, C., W. J. Ellison, L. Eymard, K. Lamkaouchi, C. Prigent, G. Delbos, A. Balana, and S. A. Boukabara (1998), Impact of new permittivity measurements on sea-surface emissivity modelling in microwaves, Radio Sci., 33, 649–667.

[12] Meisner T., and FJ Wentz, (2004), The complex dielectric constant of pure and sea water from microwave satellite observations, *IEEE Trans. Geosci. Remote Sensing,* 42, 1836- 1849.

[13] Tang, C. (1974), The effect of droplets in the air-sea transition zone on the sea brightness temperature, J. Phys. Oceanography, 4, 579-593, 1974.

[14] Schrader M., 1995: Ein dreiskalenmodell zur Berechnung der Reflektivitaet der Ozeanoberflaeche im Mikrowellenfrequenzbereich, Nr. 274, Berichte aus dem Institut fuer Meereskunde an der Universitaet zer Kiel.

[15] Wentz, F. J. (1975), A two-scale scattering model for foam-free sea microwave brightness temperature, J. Geophys. Res., 80, 3441-3446.

[16] Liu, Q., C. Simmer, and E. Ruprect (1998), Monte Carlo Simulations to Microwave Emissivity of Sea Surface, *J. Geophy. Res.*, **103**, C11, 24983-24989.

[17] Boukabara, S., F. Weng and Q. Liu, 2007: Passive Microwave Remote Sensing of Extreme Weather Events Using NOAA-18 AMSUA and MHS, IEEE Geosci. Remote Sensing, 45, 2228-2246.

[18]Weng, F., and N. C. Grody (1994), Retrieval of cloud liquid water using the special sensor microwave imager (SSM/I), *J. Geophys. Res.*, 99, 25,535–25,551.